Soft Matter

Dynamic Article Links

Cite this: *Soft Matter*, 2012, **8**, 8840

www.rsc.org/softmatter

PAPER

Two types of transitions to wrinkles in dielectric elastomers†

Jian Zhu,[a] Matthias Kollosche,[b] Tongqing Lu,[ac] Guggi Kofod*[b] and Zhigang Suo*[a]

Received 3rd May 2012, Accepted 26th June 2012
DOI: 10.1039/c2sm26034d

A membrane of a dielectric elastomer coated with compliant electrodes may form wrinkles as the applied voltage is ramped up. We present a combination of experiment and theory to investigate the transition to wrinkles using a clamped membrane subject to a constant force and a voltage ramp. Two types of transitions are identified. In type-I transition, the voltage–stretch curve is N-shaped, and flat and wrinkled regions coexist in separate areas of the membrane. The type-I transition progresses by nucleation of small wrinkled regions, followed by the growth of the wrinkled regions at the expense of the flat regions, until the entire membrane is wrinkled. By contrast, in type-II transition, the voltage–stretch curve is monotonic, and the entire flat membrane becomes wrinkled with no nucleation barrier. The two types of transitions are analogous to the first and the second order phase transitions. While the type-I transition is accompanied by a jump in the vertical displacement, type-II transition is accompanied by a continuous change in the vertical displacement. Such transitions may enable applications in muscle-like actuation and energy harvesting, where large deformation and large energy of conversion are desired.

Introduction

A membrane of a dielectric elastomer is a deformable capacitor. Subject to a tensile force in its plane, the membrane increases its area, reduces its thickness, and amplifies its capacitance. Large deformation can also be induced by applying a voltage through the thickness of the membrane. The last decade has seen the intense development of this robust electromechanical transduction as muscle-like actuators for robots,[1,2] optics,[3–6] bioengineering,[7] human–computer interfaces,[8,9] and dynamic pattern formation on curved surfaces.[10] Also under development are muscle-like generators to harvest energy from animal movements and ocean waves.[11–14]

Dielectric elastomers achieve large voltage-induced deformation by operating on the verge of instability. In a transducer, a membrane of a dielectric elastomer is sandwiched between two compliant electrodes. When the electrodes are subject to a voltage, the positive and negative charges spread on the two surfaces of the membrane, causing the membrane to reduce in thickness and expand in area. As the thickness decreases, the electric field increases. If this positive feedback prevails over the strain-stiffening of the elastomer, the membrane becomes unstable and thins down drastically. This pull-in instability often leads to electric breakdown, and has been considered as a mode of failure.[15–19] A suitably designed transducer, however, can be operated on the verge of the pull-in instability, leading to giant voltage-induced deformation prior to electric breakdown.[20,21] An acrylic elastomer has been shown to achieve voltage-induced expansion in area by 158% with a membrane biaxially prestretched and fixed to a rigid frame,[22] by 260% with a membrane constrained by two rigid clamps,[23] by 488% with a membrane subject to equal-biaxial dead loads,[24] and by 1689% with a membrane mounted in a chamber of compressed air.[25] The voltage-induced deformation measured experimentally agrees remarkably well with that predicted theoretically.[26]

The pull-in instability can also lead to electromechanical phase transitions. A prestretched membrane under a voltage is observed to deform into coexistent regions of two kinds, one being flat and the other being wrinkled.[27] This experimental observation has been interpreted theoretically as follows.[28,29] The membrane is thick in the flat regions and thin in the wrinkled regions. At a certain voltage, localized regions of the membrane undergo the pull-in instability and become thin. The thickness of the thin regions is stabilized by the steep strain-stiffening of the elastomer, so that the thin regions survive the pull-in instability without electric breakdown, and coexist with the thick regions. The deformation of the thin regions is constrained by the surrounding thick regions, causing the thin regions to form wrinkles. As more charge is supplied to the membrane, the thin regions enlarge at the expense of the thick regions, until the entire

[a]*School of Engineering and Applied Sciences, Kavli Institute of Bionano Science and Technology, Harvard University, Cambridge, MA 02138, USA. E-mail: suo@seas.harvard.edu*
[b]*ACMP, Institute of Physics and Astronomy, University of Potsdam, Karl-Liebknecht-Strasse 24-25, 14476 Potsdam, Germany. E-mail: guggi.kofod@gmail.com*
[c]*State Key Lab for Strength and Vibration of Mechanical Structures, The International Center of Applied Mechanics, School of Aerospace Engineering, Xi'an Jiaotong University, Xi'an 710049, China*
† Electronic supplementary information (ESI) available. See DOI: 10.1039/c2sm26034d

membrane becomes thin. The phenomenon is analogous to a liquid-to-vapor phase transition.

The electromechanical phase transition can be markedly affected by how mechanical loads are applied. For a dielectric elastomer under a uniaxial force, the electromechanical phase transition is predicted to occur at an electric field above the electric-breakdown strength of existing dielectric elastomers.[30] By contrast, the electromechanical phase transition is predicted to occur readily in a tubular balloon, in which bulged and unbulged sections can coexist.[31] The bulging transition dramatically amplifies electromechanical energy conversion. Energy converted in an electromechanical cycle consisting of unbulged and bulged states is thousands of times that in an electromechanical cycle consisting of only unbulged states. These theoretical predictions, however, have not been ascertained by experiments.

During a study of clamped membranes (Fig. 1), we note that many membranes under combined force and voltage form wrinkles prior to electric breakdown.[23] Our previous paper is preoccupied with achieving large voltage-induced deformation by averting various modes of failure, and does not dwell on the observation of wrinkles. Here we focus on the conditions that lead to the formation of the wrinkles. On closer examination of the videos of the experiments, we observe that membranes of different prestretches form wrinkles by two types of transitions. In type-I transition, wrinkles nucleate in small regions of a flat membrane, followed by the growth of the wrinkled regions (Video 1†). In type-II transition, wrinkles form simultaneously throughout a flat membrane without a nucleation barrier (Video 2†). We also observe that some membranes fail by electric breakdown when the membranes are still flat (Video 3†). These observations are described in some detail in this paper, and interpreted with a theoretical model. We show that the two types

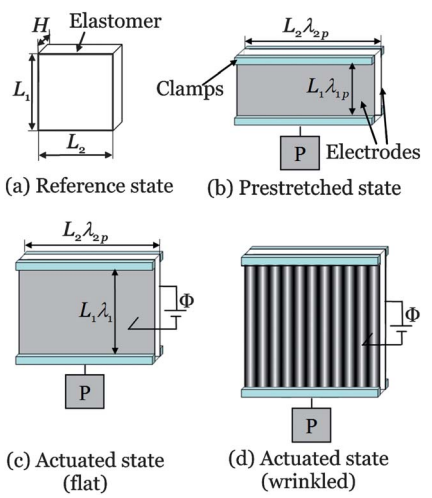

Fig. 1 An experimental setup to observe the transition to wrinkles. (a) In the reference state, a membrane of a dielectric elastomer is subject to no force and voltage. (b) In the prestretched state, constrained by rigid clamps and subject to a force P, the membrane has stretches λ_{1p} and λ_{2p}. The membrane is then coated with compliant electrodes on both surfaces. (c) In an actuated state, subject to both the force P and voltage Φ, the membrane expands in the vertical direction to a stretch λ_1. When the voltage is small, the membrane is flat. (d) When the voltage is large, the membrane is wrinkled.

of transitions are analogous to the first and the second order phase transitions. While the type-I transition is accompanied by a jump in the vertical displacement, the type-II transition is accompanied by a continuous change in the vertical displacement. Such transitions may enable applications in muscle-like actuation and energy harvesting, where large deformation and large energy of conversion are desired.

Two types of transitions to wrinkles

Following our previous work,[23] we conducted experiments with clamped membranes of a dielectric elastomer, the acrylic VHB 4905 (3 M), thickness $H = 0.5$ mm, sandwiched between carbon–grease electrodes (Fig. 1). In the reference state, the membrane is unstretched and uncharged, and is of height L_1 and length L_2. In a prestretched state, the membrane is pulled in the horizontal and vertical directions such that the height and the length of the membrane become $\lambda_{1p}L_1$ and $\lambda_{2p}L_2$. Rigid clamps are fixed to the membrane at the top and bottom edges at both sides of the stretched film. The confined area is covered with a mixture of silicone oil and carbon black to establish a homogenous and highly conductive surface electrode. Electric leads are attached to the plastic frame and connected to the electrodes to enable electric charging. The sample is then released and loaded in a tensile tester (Zwick/Roell GmbH & Co. KG, Germany) equipped with a 10 N load cell. The initial vertical length $\lambda_{1p}L_1$ is restored, and the sample is allowed to settle by viscoelastic relaxation for at least 20 minutes before the mechanical force P is noted. A self-programmed feedback loop within the measurement environment of the tensile tester is activated to enable a continuous length-adjustment of the sample to keep the force constant. In the prestretched state, the transverse length ($\lambda_{2p}L_2$) is 10 cm, which is 10 times the initial vertical length ($\lambda_{1p}L_1$). To keep the sample under clamped conditions, one needs to make the transverse length much larger than the vertical length. In an actuated state, while the force P is kept constant, a voltage Φ is applied between the two electrodes at a ramp rate of 50 V s^{-1} using a high voltage generator (HCP 35–35000, FUG Elektronik GmbH). When the voltage is small, the membrane is flat and elongates vertically. When the voltage is large, the membrane either suffers electric breakdown while still being flat, or forms wrinkles prior to electric breakdown.

We observe two types of transitions to wrinkles in membranes of different prestretches. In type-I transition, wrinkles nucleate in small regions of a flat membrane, followed by the growth of the wrinkled regions at the expense of the flat regions, until the entire membrane is wrinkled (Fig. 2). Video 1,† as well as a sequence of still images (Fig. 3), shows the sequence of the states of a membrane of prestretches {2,4} as the voltage ramps up. In the prestretched state, $\Phi = 0$, the membrane is flat, and the horizontal markings are due to the brushed carbon grease (Fig. 3a). The left and the right edges of the membrane curve in, confirming that the prestretches cause a horizontal tensile stress in the middle portion of the membrane. As the voltage ramps up, the membrane elongates in the vertical direction, and the left and the right edges become less curved and straighten up, indicating that the horizontal tensile stress is gradually relieved. When the voltage is small, the membrane remains flat. When the voltage reaches a value of about 3750 V, wrinkles nucleate in the upper

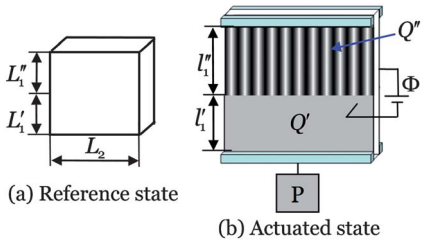

Fig. 2 Under certain conditions, flat and wrinkled regions coexist in a membrane. As more charge is supplied to the membrane, the wrinkled region enlarges at the expense of the flat region, until the entire membrane is wrinkled. (a) In the reference state, the flat and the wrinkled regions are of heights L_1' and L_1'', respectively. (b) In the actuated state, the two regions are of heights l_1' and l_1'' and charges Q' and Q''.

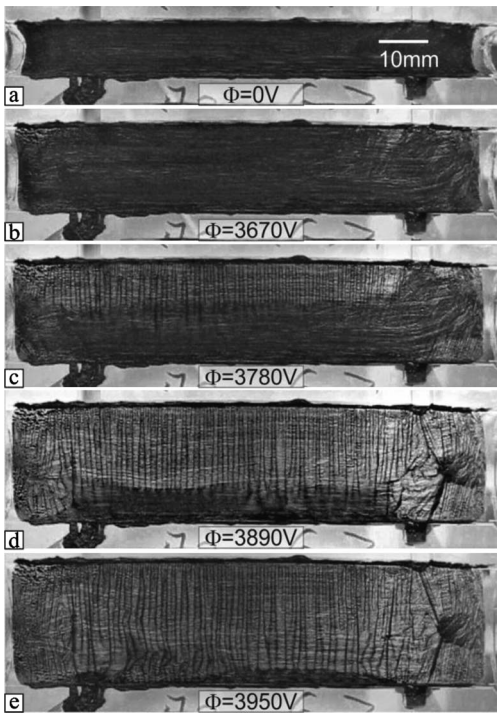

Fig. 3 Experimental observation of a transition from a flat state to a wrinkled state. (a) The membrane is in the prestretched state ($\lambda_{1p} = 2$ and $\lambda_{2p} = 4$), subject to no voltage. (b) The membrane is subject to a voltage and is still flat, just before wrinkles nucleate. Wrinkles nucleate at a voltage about $\Phi \approx 3750$ V. (c and d) The wrinkled region enlarges at the expense of the flat region. (e) The entire membrane is wrinkled.

region of the membrane. The wrinkled regions spread across the entire membrane within a time of about 5 seconds, during which the voltage ramps up about 250 V. That is, the flat membrane transforms into the wrinkled membrane by nucleation and growth within a narrow range of voltage. Type-I transition is accompanied by a jump in the vertical displacement.

In type-II transition, wrinkles form simultaneously throughout a flat membrane without a nucleation barrier. Video 2† shows the sequence of the states of a membrane of prestretches {5,5} as the voltage ramps up. The flat membrane transforms into the wrinkled membrane at a voltage of 2750 V. The transition occurs throughout the membrane simultaneously, rather than by nucleation and growth. The type-II transition is accompanied by a continuous change in the vertical displacement.

We also observe that some membranes fail by electric breakdown when the membranes are still flat. Video 3† shows the sequence of the states of a membrane of prestretches {1,2} as the voltage ramps up. The membrane elongates in the vertical direction, but remains flat. The membrane fails by electric breakdown without forming any wrinkles.

We interpret our experimental observations by applying a theory of electromechanical phase transition.[28–31] For a membrane of prestretches $\{\lambda_{1p},\lambda_{2p}\}$, as the voltage Φ ramps up, the membrane is in a succession of states of equilibrium, represented by a curve in the voltage–charge diagram (Fig. 4). Each point on the curve corresponds to a state of equilibrium of the membrane under a given voltage. The curve consists of two branches: one corresponding to a flat membrane and the other to a wrinkled membrane. When the voltage is small, the membrane is flat and subject to a horizontal tensile stress. As the voltage increases, the membrane reduces in thickness and expands in area. However, the length of the membrane in the horizontal direction is constrained by the clamps, so that the horizontal tensile stress reduces as the voltage increases. At a certain value of the voltage, represented by an open circle in Fig. 4, the horizontal stress vanishes. The loss of transverse tension causes the membrane to form wrinkles. After the membrane forms wrinkles, the horizontal stress may be set to zero.

For a membrane of small prestretches, the voltage–charge curve is N-shaped—going up, down, and up again (Fig. 4a). When the charge is small, the membrane is flat, and the voltage needed to maintain the charge increases with the charge. When

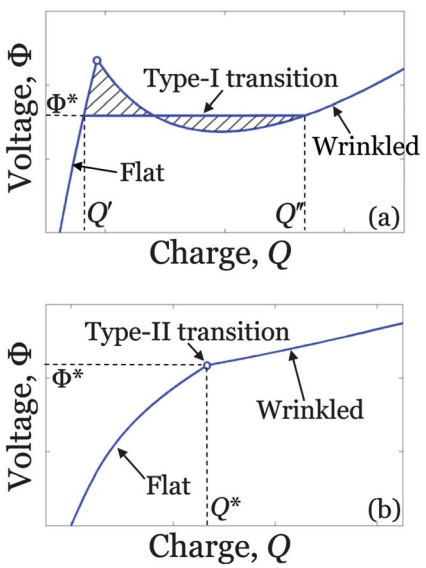

Fig. 4 For a membrane of given prestretches λ_{1p} and λ_{2p}, as the voltage Φ varies, the membrane is in a succession of states of equilibrium, represented by a curve in the voltage–charge diagram. The curve has two branches, one corresponding to a flat membrane and the other to a wrinkled membrane. (a) In a type-I transition, the voltage–charge curve is N-shaped, and a flat region and a wrinkled region can coexist over a range of the charge from Q' to Q''. (b) In a type-II transition, the voltage–charge curve is monotonic, and the entire membrane changes from a flat state to a wrinkled state at a specific value of the charge Q^*.

the charge is large enough, the membrane may form wrinkles, and the elastomer thins down appreciably. The electric field through the thickness is very high, so the voltage needed to maintain the charge starts to decrease. As a result, the voltage reaches a peak. Upon approaching the extension limit of the polymer, the membrane stiffens steeply, and the voltage–stretch curve goes up again. If the combination of the two curves is N-shaped, a flat region and a wrinkled region can coexist over a range of the charge at the voltage of transition. This is graphically represented by the horizontal line that makes the two shaded regions have the same area, a construction analogous to the Maxwell rule in thermodynamic phase transition.[28] This behavior corresponds to the type-I transition. By contrast, for a membrane of large prestretches, the voltage–charge curve is monotonic (Fig. 4b). The entire membrane may change from a flat state to a wrinkled state continuously, at a specific value of the voltage. This behavior corresponds to the type-II transition.

The two types of transitions to wrinkles are analogous to the first and the second order phase transitions. While the type-I transition is accompanied by a jump in the charge, the type-II transition is accompanied by a gradual increase in the charge. Our experimental setup allows us to observe the jump in the vertical displacement in type-I transition, as well as the gradual increase in the vertical displacement in a type-II transition.

Theory of electromechanical phase transition

To compare the experimental observations to the above model quantitatively, we analyze the model by using a theory of dielectric elastomer. The part of the theory essential to this work is briefly summarized here; for more details see a recent review.[32] The undeformed and uncharged membrane is of thickness H and lengths L_1 and L_2. When the membrane is subject to voltage Φ through the thickness and forces P_1 and P_2 in the two directions in the plane, the membrane deforms to thickness h and lengths l_1 and l_2, and the two surfaces of the membrane have charges $\pm Q$. Define the stresses by $\sigma_1 = P_1/(l_2h)$ and $\sigma_2 = P_2/(l_1h)$, stretches by $\lambda_1 = l_1/L_1$ and $\lambda_2 = l_2/L_2$, electric field by $E = \Phi/h$ and electric displacement by $D = Q/(l_1l_2)$. We adopt the model of ideal dielectric elastomer. The elastomer is taken to be incompressible, $L_1L_2H = l_1l_2h$, and the electric displacement is taken to be linear in the electric field,

$$D = \varepsilon E \tag{1}$$

where the permittivity ε is a material constant independent of the state of deformation and charge. The electric field induces deformation through an effective stress (known as the Maxwell stress). Because the elastomer is taken to be incompressible, the effect of the Maxwell stress is exactly the same as that of equal biaxial tensile stresses with an amplitude of εE^2.[32] The combination of the Maxwell stress and the applied mechanical stress stretches the membrane:

$$\sigma_1 + \varepsilon E^2 = \lambda_1 \frac{\partial W(\lambda_1, \lambda_2)}{\partial \lambda_1}, \tag{2}$$

$$\sigma_2 + \varepsilon E^2 = \lambda_2 \frac{\partial W(\lambda_1, \lambda_2)}{\partial \lambda_2}. \tag{3}$$

where $W(\lambda_1,\lambda_2)$ is the Helmholtz free energy per unit volume due to stretching. Eqn (1)–(3) constitute the equations of state for the ideal dielectric elastomer. See Suo[32] for the detailed derivation of eqn (2) and (3).

Keplinger *et al.* show the slow viscoelastic drift of a DEA in the pull-in instability and breakdown failure mode, when the actuator is subject to stepwise voltages.[33] It is found that at a certain value of voltage, wrinkled regions may grow, slowly driving the actuator into failure. Viscoelasticity does play an important role in electromechanical behavior of the dielectric elastomer actuator, especially when the actuator is subject to a static or stepwise voltage, as shown in ref. 33. For simplicity, in the current analysis we use an elastic model to illustrate the two types of transitions to wrinkles. How viscoelasticity affects these transitions to wrinkles deserves further study.

To account for the strain-stiffening of the elastomer, we adopt the Gent model:[34]

$$W(\lambda_1, \lambda_2) = -\frac{\mu J_{\lim}}{2} \log\left(1 - \frac{\lambda_1^2 + \lambda_2^2 + \lambda_1^{-2}\lambda_2^{-2} - 3}{J_{\lim}}\right), \tag{4}$$

where μ is the small-strain shear modulus, and $J_{\lim}$ is a material constant related to the limiting stretch. When deformation is small, $(\lambda_1^2 + \lambda_2^2 + \lambda_1^{-2}\lambda_2^{-2} - 3)/J_{\lim} \to 0$, the Taylor expansion of (4) recovers the neo-Hookean model. When deformation approaches the extension limit, $(\lambda_1^2 + \lambda_2^2 + \lambda_1^{-2}\lambda_2^{-2} - 3)/J_{\lim} \to 1$, the elastomer stiffens steeply. In calculations, we use the following values for the material parameters: $\mu = 50$ kPa, $\varepsilon = 4.65 \times 8.85 \times 10^{-12}$ F m^{-1} and $J_{\lim} = 140$.[23]

We signify quantities specific to a flat membrane by the single prime, and quantities specific to a wrinkled membrane by the double prime (Fig. 2). In a flat membrane, the horizontal stretch is constrained by the clamps and keeps the constant value of the prestretch, $\lambda_2' = \lambda_{2p}$, but the vertical stretch λ_1' increases as the voltage ramps up. The vertical stress is $\sigma_1' = \lambda_1' P/(L_2H)$ and the electric field is $E' = (\Phi/H)\lambda_1'\lambda_{2p}$. Eqn (2) becomes

$$\frac{P}{L_2H}\lambda_1' + \varepsilon\left(\frac{\Phi}{H}\right)^2\left(\lambda_1'\lambda_{2p}\right)^2 = \lambda_1' \frac{\partial W\left(\lambda_1', \lambda_{2p}\right)}{\partial \lambda_1'}. \tag{5}$$

This equation determines the vertical stretch λ_1' of the flat membrane when P and Φ are given. In particular, when $\Phi = 0$, (5) relates the vertical prestretch λ_{1p} to the applied force P.

In a wrinkled membrane, the horizontal stress vanishes, $\sigma_2'' = 0$, and both the vertical stretch λ_1'' and the horizontal stretch λ_2'' increase as the voltage ramps up. Note that $\lambda_2'' > \lambda_{2p}$ due to wrinkles. The vertical stress is $\sigma_1'' = \lambda_1'' P/(L_2H)$ and the electric field is $E'' = (\Phi/H)\lambda_1''\lambda_2''$. Eqn (2) and (3) become

$$\frac{\lambda_1'' P}{L_2H} + \varepsilon\left(\frac{\Phi}{H}\right)^2(\lambda_1''\lambda_2'')^2 = \lambda_1'' \frac{\partial W(\lambda_1'', \lambda_2'')}{\partial \lambda_1''}, \tag{6}$$

$$\varepsilon\left(\frac{\Phi}{H}\right)^2(\lambda_1''\lambda_2'')^2 = \lambda_2'' \frac{\partial W(\lambda_1'', \lambda_2'')}{\partial \lambda_2''}. \tag{7}$$

The two equations determine the stretches λ_1'' and λ_2'' of the wrinkled membrane when P and Φ are given.

We formulate the condition under which flat and wrinkled regions coexist in a membrane following a similar approach described before.[28–31] In the reference state, the flat and the

wrinkled regions are of heights $L_1^{'}$ and $L_1^{''}$, respectively. In an actuated state, the two regions are of heights $l_1^{'}$ and $l_1^{''}$ and charges $Q^{'}$ and $Q^{''}$. The membrane, along with the mechanisms that apply the voltage and force, forms a composite thermodynamic system. Under the isothermal condition, the composite reaches a state of equilibrium when the Helmholtz free energy of the composite is stationary. The Helmholtz free energy of the membrane consists of both the elastic energy due to stretching and the dielectric energy: $L_1^{'}L_2H(W(\lambda_1^{'},\lambda_2^{'}) + (D^{'})^2/(2\varepsilon)) + L_1^{''}L_2H(W(\lambda_1^{''},\lambda_2^{''}) + (D^{''})^2/(2\varepsilon))$. The potential energy of the mechanism that applies the voltage is $-\Phi(Q^{'} + Q^{''})$. The potential energy of the mechanism that applies the force is $-P(l_1^{'} + l_1^{''})$. The sum of these contributions gives the Helmholtz free energy of the composite. Recall that $L_1^{'} + L_1^{''} = L_1$, $l_1^{'} = \lambda_1^{'}L_1^{'}$, $\lambda_2^{'} = \lambda_{2p}$, $l_1^{''} = \lambda_1^{''}L_1^{''}$, $Q^{'} = D^{'}\lambda_1^{'}\lambda_2^{'}L_1^{'}L_2$ and $Q^{''} = D^{''}\lambda_1^{''}\lambda_2^{''}L_1^{''}L_2$. Under constant voltage Φ and force P, the Helmholtz free energy of the composite is a function of six independent variables: $D^{'}$, $\lambda_1^{'}$, $D^{''}$, $\lambda_1^{''}$, $\lambda_2^{''}$, $L_1^{'}$. The free energy function is stationary when the composite reaches a state of equilibrium. Setting the partial derivatives of the free energy with respect to the independent variables to zero, we obtain six equations of equilibrium, five of which recover the equations of state in the flat and wrinkled regions. The sixth equation results from setting the partial derivative of the free energy of the composite with respect to $L_1^{'}$ to zero, giving

$$W\left(\lambda_1^{'},\lambda_{2p}\right) - \frac{P}{L_2H}\lambda_1^{'} - \frac{\varepsilon}{2}\left(\frac{\Phi}{H}\right)^2\left(\lambda_1^{'}\lambda_{2p}\right)^2 = W(\lambda_1^{''},\lambda_2^{''}) - \frac{P}{L_2H}\lambda_1^{''} - \frac{\varepsilon}{2}\left(\frac{\Phi}{H}\right)^2(\lambda_1^{''}\lambda_2^{''})^2. \quad (8)$$

This equation is the condition for the flat and the wrinkled regions to equilibrate in the membrane. The condition is readily understood: in equilibrium, the Helmholtz free energy of the composite per unit length must be equal in the flat and the wrinkled regions. See Huang and Suo[30] for the detailed derivation of (8).

When the prestretches $\{\lambda_{1p},\lambda_{2p}\}$ are given, eqn (5)–(8) determine the quantities associated with the coexistent flat and wrinkled regions: Φ, $\lambda_1^{'}$, $\lambda_1^{''}$ and $\lambda_2^{''}$. For a membrane of small prestretches, a solution exists with $\lambda_2^{''} > \lambda_{2p}$, corresponding to a type-I transition. However, for a membrane of large prestretches, we only can obtain a solution with $\lambda_1^{'} = \lambda_1^{''}$ and $\lambda_2^{''} = \lambda_{2p}$, corresponding to a type-II transition.

The voltage of transition Φ^* is solved for membranes of various prestretches (Fig. 5). Below the curve, the entire membrane is flat. Above the curve, the entire membrane is wrinkled. The curve—the phase boundary—consists of two parts. The solid part corresponds to the type-I transition, while the dashed part corresponds to the type-II transition. The vertical line corresponds to the condition of no applied force, $P = 0$.

The calculated state of the membrane can be represented in the $\Phi - \lambda_1$ diagrams (Fig. 6). Each diagram is for a specific value of the horizontal prestretch λ_{2p}, as marked in the diagram. Within a diagram, each curve is the voltage–stretch curve under a constant force P, with the corresponding value of λ_{1p} read from the intersection of the curve and the horizontal axis. The left part of the curve corresponds to a flat membrane, and the right part of the curve corresponds to a wrinkled membrane. A horizontal line

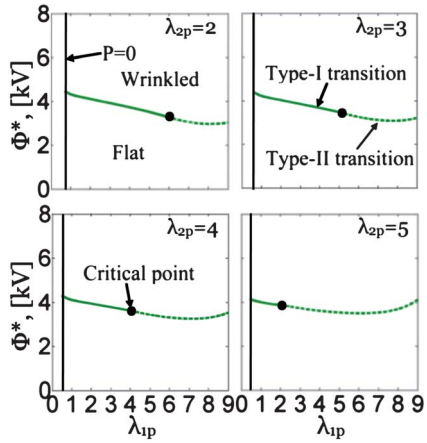

Fig. 5 The voltage of transition depends on the prestretches λ_{1p} and λ_{2p}. The entire membrane is flat when the voltage is below the curve and is wrinkled when the voltage is above the curve. The solid curve corresponds to the type-I transition and the dashed curve corresponds to the type-II transition.

represents a membrane of coexistent flat and wrinkled regions, undergoing the type-I transition. An open circle represents an entire membrane changing from a flat state to a wrinkled state, undergoing the type-II transition. For a membrane of a fixed horizontal prestretch λ_{2p}, it undergoes the type-I transition when the vertical prestretch λ_{1p} is small (*e.g.*, $\lambda_{2p} = 2$ and $\lambda_{1p} = 3$), but undergoes the type-II transition when the vertical prestretch λ_{1p} is larger (*e.g.*, $\lambda_{2p} = 2$ and $\lambda_{1p} = 6$). Comparing diagrams in Fig. 6, we note that type-II transition is more likely when the membrane is under a higher value of the horizontal prestretch.

Comparison between theory and experiment

Dielectric elastomers are susceptible to electric breakdown. Here we set a representative electric breakdown field $E_{EB} = 300$ MV m^{-1}.[23]

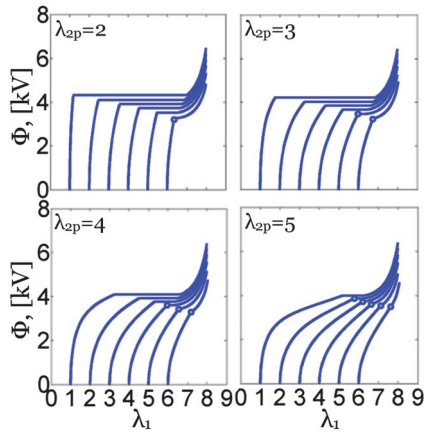

Fig. 6 For a membrane with given prestretches λ_{1p} and λ_{2p}, as the voltage Φ varies, the membrane is in a succession of states of equilibrium, represented by a curve in the voltage–stretch diagram. The value of λ_{2p} is marked in each diagram and the value of λ_{1p} can be read from the intersection of the curve and the horizontal axis. A horizontal line represents a membrane of coexistent flat and wrinkled regions (type-I transition). An open circle represents an entire membrane changing from a flat state to a wrinkled state (type-II transition).

In each voltage–stretch diagram, in addition to a curve representing the states of equilibrium for a membrane of given prestretches $\{\lambda_{1p},\lambda_{2p}\}$, the conditions of electric breakdown are represented by two curves: the dashed curve assumes that electric breakdown occurs when the membrane is flat, and the solid curve assumes that electric breakdown occurs when the membrane is wrinkled (Fig. 7). Depending on how electric breakdown terminates the voltage–stretch curve, we identify several kinds of representative behavior. The first kind is that the voltage–stretch curve exhibits type-I transition, and both the flat and the wrinkled regions are below the breakdown condition, so that coexistent flat and wrinkled regions are observable (Video 1†). The second kind is that the voltage–stretch curve is monotonic, and both the flat and the wrinkled regions are below the breakdown condition, so that the type-II transition is observable (Video 2†). The third kind is that the voltage–stretch curve exhibits the type-I transition, the flat region is below the breakdown condition but the wrinkled regions suffer breakdown, so that transitions are not observable and the failure occurs when essentially the entire membrane is still flat (Video 3†). The fourth kind is that the voltage–stretch curve is monotonic, and the flat region suffers electric breakdown prior to the transition to wrinkles. The experimental observations for the third and the fourth behavior may appear to be similar—that is, the membrane fails before forming wrinkles. However, they correspond to different sequences of events, and occur to membranes of different prestretches.

We now compare the theory to the experiment quantitatively (Fig. 8). The black data points are the experimental data. For a membrane of prestretches $\lambda_{1p} = 2$ and $\lambda_{2p} = 4$ (Fig. 8a), wrinkles nucleate in small regions, and then spread across the entire membrane. During the transition to wrinkles, the vertical displacement greatly increases (type-I transition). The fully wrinkled membrane sustains further increase in voltage before electric breakdown. For a membrane of prestretches $\lambda_{1p} = 5$ and $\lambda_{2p} = 5$ (Fig. 8b), our theory is qualitatively consistent with the experimental observation. During the transition to wrinkles, the vertical displacement is nearly unchanged (type-II transition). The fully wrinkled membrane sustains further increase in voltage before electric breakdown. For a membrane of prestretches $\lambda_{1p} = 1$ and $\lambda_{2p} = 2$ (Fig. 8c), the membrane is still flat upon electric breakdown. As illustrated in Fig. 7c, the membrane may fail in a flat state, due to that the wrinkled state at the transition line suffers electric breakdown. Another possible reason may be as follows. The voltage–stretch curve is N-shaped (Fig. 8c). If the peak voltage is much larger than the predicted voltage of transition, the large barrier may make wrinkles difficult to nucleate. As a result, the membrane may suffer snap-through instability when the voltage reaches the local peak A. The membrane may fail at the flat state because the wrinkled state B suffers electric breakdown.

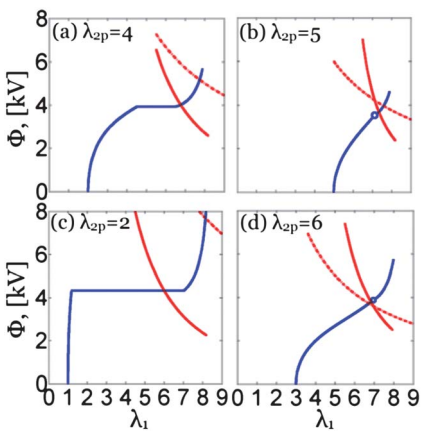

Fig. 7 On each voltage–stretch diagram, in addition to the blue curve which represents the states of equilibrium corresponding to a membrane of given prestretches λ_{1p} and λ_{2p}, the conditions of electric breakdown are represented by two red curves: the dashed curve assumes that breakdown occurs when the membrane is flat, and the solid curve assumes that electric breakdown occurs when the membrane is wrinkled. Depending on where these curves intersect, several kinds of representative behavior are identified. (a) The voltage–stretch curve exhibits a type-I transition, and both the flat and the wrinkled regions are below the breakdown conditions, so that coexistent flat and wrinkled regions are observable. (b) The voltage–stretch curve is monotonic and exhibits a type-II transition, since both the flat and the wrinkled regions are below the breakdown conditions. (c) The voltage–stretch curve exhibits a type-I transition, the flat region is below the breakdown condition but the wrinkled region suffers electric breakdown, so that coexistent regions are not observable. (d) The voltage–stretch curve is monotonic and the flat region suffers electric breakdown.

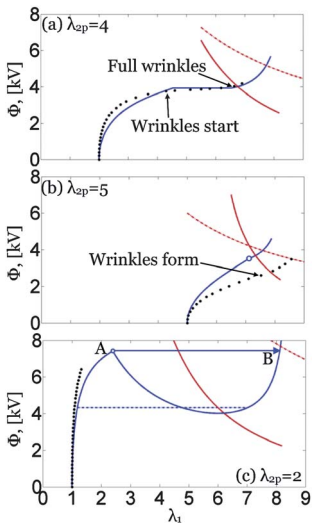

Fig. 8 Comparison between experiment and theory. The black data points are experimental data. The blue curves are theoretical predictions using $\mu = 50$ kPa and $J_{lim} = 140$. Also plotted are the predicted conditions of electric breakdown in wrinkled regions (solid red curves), and in flat regions (dashed red curves). (a) For a membrane of prestretches $\lambda_{1p} = 2$ and $\lambda_{2p} = 4$, wrinkles nucleate in small regions and then spread across the entire membrane, while the vertical stretch greatly increases (type-I transition). The fully wrinkled membrane sustains further increase in voltage before electric breakdown. Before the wrinkles start, the time between two successive experimental data points is 4 s. However, between the point when the wrinkles start (at $\Phi = 3750$ V) and the point for the full wrinkles (at $\Phi = 4000$ V), the time between two successive points is not constant (about 1–2 s). The coexistent regions last about 5 s. (b) For a membrane of prestretches $\lambda_{1p} = 5$ and $\lambda_{2p} = 5$, wrinkles form at a specific value of the vertical stretch (type-II transition). The fully wrinkled membrane sustains further increase in voltage before electric breakdown. (c) For a membrane of prestretches $\lambda_{1p} = 1$ and $\lambda_{2p} = 2$, the membrane is still flat upon electric breakdown. In (b) and (c), the time between two successive experimental data points is 4 s.

Concluding remarks

A membrane of a dielectric elastomer may form wrinkles as the applied voltage ramps up. We identify two types of transitions. In type-I transition, the voltage–stretch curve is N-shaped, and the flat and the wrinkled regions coexist in the membrane. The type-I transition progresses by nucleation of small wrinkled regions, followed by the growth of the wrinkled regions at the expense of the flat regions, until the entire membrane is wrinkled. By contrast, in type II transition, the voltage–stretch curve is monotonic, and the entire flat membrane becomes wrinkled with no nucleation barrier. In the existing literature, coexistent flat and wrinkled states have been difficult to study experimentally because the observed patterns of wrinkled regions are complicated, or because wrinkled states often suffer electric breakdown. Here the simple setup – a clamped membrane – permits a combined experimental and theoretical investigation.

Practical designs of dielectric elastomer transducers usually involve constraints in one form or another, and wrinkles are often observed in actuated states. As we have shown, membranes may survive the formation of wrinkles without electric breakdown, and wrinkled states may achieve large voltage-induced deformation. Whether they do form wrinkles without electric breakdown and achieve large voltage-induced deformation depends on the design of the transducers. It is hoped that an understanding of the electromechanical phase transition will enable applications in muscle-like actuation and energy harvesting, where large deformation and large energy of conversion are desired.

Acknowledgements

The work of JZ and ZGS is supported by ARO (W911NF-09-1-0476), DARPA (W911NF-10-1-0113), and MRSEC. MK and GK thank the German Federal Ministry of Education and Research (BMBF) for support *via* grant no. 03X5511 "KompAkt" (WING-NanoFutur). TQL is supported by China Scholarship Council as a visiting scholar for two years at Harvard University. ZGS acknowledges a sabbatical leave at the Karlsruhe Institute of Technology funded by the Alexander von Humboldt Award and by Harvard University.

References

1 Q. B. Pei, R. Pelrine, S. Stanford, R. Kornbluh and M. Rosenthal, *Synth. Met.*, 2003, **135**, 129–131.
2 G. Kovacs, L. Düring, S. Michel and G. Terrasi, *Sens. Actuators, A*, 2009, **155**, 299–307.
3 M. Aschwanden and A. Stemmer, *Opt. Lett.*, 2006, **31**, 2610–2612.
4 S. Döring, M. Kollosche, T. Rabe, J. Stumpe and G. Kofod, *Adv. Mater.*, 2011, **23**, 4265–4269.
5 M. Kollosche, S. Döring, J. Stumpe and G. Kofod, *Opt. Lett.*, 2011, **36**, 1389–1391.
6 F. Carpi, G. Frediani, S. Turco and D. De Rossi, *Adv. Funct. Mater.*, 2011, **21**, 4002–4008.
7 S. Akbari and H. R. Shea, *J. Micromech. Microeng.*, 2012, **22**, 045020.
8 Z. B. Yu, W. Yuan, P. Brochu, B. Chen, Z. T. Liu and Q. B. Pei, *Appl. Phys. Lett.*, 2009, **95**, 192904.
9 M. Rosenthal and A. Cheng, *WW-EAP Newsletter*, 2011, **13**, 2.
10 Q. M. Wang, M. Tahir, J. F. Zang and X. H. Zhao, *Adv. Mater.*, 2012, **24**, 1947–1951.
11 T. Mckay, B. M. O'Brien, E. Calius and I. A. Anderson, *Appl. Phys. Lett.*, 2010, **97**, 062911.
12 R. Kaltseis, C. Keplinger, R. Baumgartner, M. Kaltenbrunner, T. F. Li, P. Mächler, R. Schwödiauer, Z. G. Suo and S. Bauer, *Appl. Phys. Lett.*, 2011, **99**, 162904.
13 K. Ahnert, M. Abel, M. Kollosche, P. J. Jørgensen and G. Kofod, *J. Mater. Chem.*, 2011, **21**, 14492–14497.
14 R. D. Kornbluh, R. Pelrine, H. Prahlad, A. Wong-Foy, B. McCoy, S. Kim, J. Eckerle and T. Low, *MRS Bull.*, 2012, **37**, 246–253.
15 R. E. Pelrine, R. D. Kornbluh and J. P. Joseph, *Sens. Actuators, A*, 1998, **64**, 77–85.
16 M. Wissler and E. Mazza, *Sens. Actuators, A*, 2005, **120**, 184–192.
17 E. M. Mockensturm and N. Goulbourne, *Int. J. Nonlinear Mech.*, 2006, **41**, 388–395.
18 X. H. Zhao and Z. G. Suo, *Appl. Phys. Lett.*, 2007, **91**, 061921.
19 A. N. Norris, *Appl. Phys. Lett.*, 2008, **92**, 026101.
20 X. H. Zhao and Z. G. Suo, *Phys. Rev. Lett.*, 2010, **104**, 178302.
21 S. J. A. Koh, T. F. Li, J. X. Zhou, X. H. Zhao, W. Hong, J. Zhu and Z. G. Suo, *J. Polym. Sci., Part B: Polym. Phys.*, 2011, **49**, 504–515.
22 R. Pelrine, R. Kornbluh, Q. B. Pei and J. Joseph, *Science*, 2000, **287**, 836–839.
23 M. Kollosche, J. Zhu, Z. G. Suo and G. Kofod, *Phys. Rev. E: Stat., Nonlinear, Soft Matter Phys.*, 2012, **85**, 051801.
24 J. S. Huang, T. F. Li, C. C. Foo, J. Zhu, D. R. Clarke and Z. G. Suo, *Appl. Phys. Lett.*, 2012, **100**, 041911.
25 C. Keplinger, T. F. Li, R. Baumgartner, Z. G. Suo and S. Bauer, *Soft Matter*, 2012, **8**, 285–288.
26 T. Q. Lu, J. S. Huang, C. Jordi, G. Kovacs, R. Huang, D. R. Clarke and Z. G. Suo, *Soft Matter*, 2012, **8**, 6167–6173.
27 J. S. Plante and S. Dubowsky, *Int. J. Solids Struct.*, 2006, **43**, 7727–7751.
28 X. H. Zhao, W. Hong and Z. G. Suo, *Phys. Rev. B: Condens. Matter Mater. Phys.*, 2007, **76**, 134113.
29 J. X. Zhou, W. Hong, X. H. Zhao, Z. Q. Zhang and Z. G. Suo, *Int. J. Solids Struct.*, 2008, **45**, 3739–3750.
30 R. Huang and Z. G. Suo, *Proc. R. Soc. London, Ser. A*, 2011, **468**, 1014–1040.
31 T. Q. Lu and Z. G. Suo, *Acta Mechanica Sinica*, DOI: 10.1007/s10409-012-0091-x.
32 Z. G. Suo, *Acta Mech. Solida Sin.*, 2010, **23**, 549–578.
33 C. Keplinger, M. Kaltenbrunner, N. Arnold and S. Bauer, *Appl. Phys. Lett.*, 2008, **92**, 192903.
34 A. N. Gent, *Rubber Chem. Technol.*, 1996, **69**, 59–61.

